Oxidation of Alkali-Metal Atoms with Nitrous Oxide: Molecular Mechanisms from First Principles Calculations

Oksana Tishchenko, Christian Vinckier, and Minh Tho Nguyen*

Department of Chemistry, University of Leuven, Celestijnenlaan 200 F, B-3001 Leuven, Belgium

Received: June 10, 2003; In Final Form: November 10, 2003

The reactions of nitrous oxide with alkali-metal atoms were studied theoretically by means of CASSCF(11/12)/MR-MP2 calculations. Critical points on the electronic ground-state $^2A'$ potential energy surface (PES) were determined and characterized by harmonic vibrational frequencies at the CASSCF(11/12) level. The molecular mechanism is rather consistent involving in each reaction two distinct entrance channels. Small barriers of 5.9 kcal/mol for Li + N_2O, 1.6 kcal/mol for Na + N_2O, and 1.2 kcal/mol for K + N_2O are predicted for the lower energy reaction channel, which is mainly determined by the NNO bending vibrational mode ν_2. These barriers originate as a result of strong avoided crossings between the two lowest $^2A'$ PESs that gradually transform the character of the electronic ground state from a neutral to an ionic one in going from reactants to products. Along this channel, the ground-state PES is fairly isolated and the reaction is adiabatic. By way of contrast, the reaction along its higher energy channel occurs via nonadiabatic electron transfer from alkali metal to N_2O in the region of the $1^2A'/2^2A'$ conical intersection and likely contributes to the observed non-Arrhenius behavior of the reaction rates. These findings provide clarifying insights into the nature of a number of previous kinetic and spectroscopic observations.

1. Introduction

Nitrous oxide (N_2O) is a vital constituent of the Earth's atmosphere. It is known to provide the key mechanism regulating ozone concentration in stratospheric ozone layer and to participate in processes responsible for the thermal balance of the Earth.[1] Recently, there has been considerable concern about environmental issues associated with the growth of the N_2O concentration in the atmosphere as a result of human activity,[2] and in this global context, considerable efforts have been devoted to find ways of reducing anthropogenic emission of greenhouse nitrous oxide gas. Of various available proposals, the addition of alkali metals to high-temperature industrial processes or incinerators has been considered as an efficient means of destroying N_2O, thanks to large exothermicity and rapidity of the corresponding reactions.[3] As for an alternative, the catalytic decomposition on various surfaces involving a dissociative electron attachment to N_2O has also been put forward.[4] Among other applications of the title reactions is their frequent use in an *in situ* generation of alkali-metal oxides for subsequent study of spectra and reactions of these atmospherically important oxides.[5]

As is well-known, the oxidation of metal atoms with N_2O proceeds via the following reaction step (M = metal):

$$N_2O(X^1\Sigma^+) + M \rightarrow MO + N_2 \qquad (1)$$

A number of available experiments illustrate its mechanistic complexity. First, this reaction reveals a rather pronounced non-Arrhenius behavior for M = Li[6a] and M = K,[6b] in contrast to M = Na,[7] where it shows a simple Arrhenius regime in a wide temperature range and thus becomes a "kinetic standard" for the design of new experimental systems for metal reactions.[8] The appearance of non-Arrhenius behavior usually suggests an interplay of two or more reaction channels on the ground potential energy surface (PES) characterized by different Arrhenius parameters and/or a possibility of electronically nonadiabatic transitions between different PESs at higher temperatures. Some legitimate questions can then be posed: what is the molecular mechanism behind reaction 1, which PESs control the reactivity, and how do(es) the involved reaction channel(s) structurally look?

A second, no less puzzling, observation is a broad emission accompanying reaction 1 which extends through the entire visible region to near-infrared for M = Li and lies at the fringes of the visible region for heavier congeners.[9] The observed emission was tentatively ascribed to weakly bound states of covalent nature ($B^2\Pi$) of alkali-metal oxides,[9] which have been further characterized theoretically.[10] These excited states, however, are energetically unaccessible in reaction 1 under the employed experimental conditions, and such an assignment has been recently questioned.[11] If involved, how are excited states then formed here?

The present work, prompted by the questions outlined above, considers the molecular mechanism of reaction 1 on the basis of high-level *ab initio* calculations. Although there have been some earlier studies on analogous reactions of N_2O with transition metals[12] and alkaline-earth-metal atom Mg,[13] surprisingly no theoretical data, apart from our preliminary results for the N_2O + Li reaction,[14] are available on the title reactions. The paper is organized as follows: Section 2 provides a description of *ab initio* methods employed in the present work, in sections 3 and 4, we discuss the key electronic structure features of the N_2O + M reaction systems governing the reaction mechanism, and, finally, section 5 provides a summary of the work.

* To whom correspondence should be addressed. Fax: +32 (16) 32 79 92. E-mail: Minh.Nguyen@chem.kuleuven.ac.be.

10.1021/jp0307295 CCC: $27.50
Published on Web 01/22/2004

2. Computational Approach

Throughout this work, the complete active space self-consistent field (CASSCF) method[15] and the multireference second-order perturbation theory MR-MP2[16a−d] were employed. The active space selected for CASSCF computations consisted of the MOs resulting from 2p orbitals of N and O atoms, and the *n*s orbitals of the alkali metal and involved 12 active orbitals for 11 active electrons referred to hereafter as (11/12) active space, namely, in C_s symmetry:

$$[8A' - 16A', 1A'' - 4A'']^{11}$$

$$[12A' - 20A', 2A'' - 5A'']^{11}$$

$$[16A' - 24A', 3A'' - 6A'']^{11}$$

for the representation of reaction 1 with Li, Na, and K atoms, respectively, which allows a balanced description of various regions of the lower lying PESs.

Using this (11/12) active space, a full optimization of all local minima and relevant transition structures on the ground-state PES with subsequent harmonic vibrational analysis was performed at the CASSCF level. This is expected to provide a realistic representation of the topography of the ground-state PES, albeit the inclusion of dynamic correlation is still required to obtain accurate reaction barriers, which tend to be overestimated by ca. 10−12 kcal/mol at the CASSCF level.[17] Dynamic correlation effects at the key points of the PES governing the reaction mechanism were accounted for by applying the MR-MP2 theory. In these MR-MP2 calculations, all the orbitals except for 1s were correlated. Separate CASSCF calculations were also carried out as an average over several roots to rationalize the origins of the reaction barriers. To describe coupled electronic states, it is necessary, in addition to the adiabatic energies, to calculate the nonadiabatic coupling matrix elements (NACMEs), $\langle \Psi^a{}_1 | \partial/\partial Q | \Psi^a{}_2 \rangle$, where $\Psi^a{}_1$ and $\Psi^a{}_2$ are eigenvectors of the electronic Hamiltonian and Q is the internal coordinate of the molecule. In this work, the NACMEs in transition regions were evaluated applying the two- and three-point finite difference methods[18] as implemented in MOLPRO.[19]

All the geometry optimizations and frequency calculations were carried out using the GAMESS[20] program, whereas partial cross-sections of the PESs describing reaction 1 were computed using the MOLPRO program. The latter has also been employed for optimization of conical intersection (CI) structures. Unless otherwise noted, energy-minimized CI structures reported in this work were determined using a smaller (5/6) active space. A number of test calculations have subsequently been performed in the CI regions to confirm that the presence of the CI points is not sensitive to the dynamic correlation effects. Dynamic correlation in this case was accounted for by using the multiconfigurational second-order quasidegenarate pertubation theory (MCQDPT2)[16e] calculations based on state-averaged CASSCF references.

The atomic-orbital basis sets employed were of triple-ζ quality, viz., 6-311+G(d) for N, O, Li, and Na atoms, and TZV[21] supplemented with one d function ($\alpha = 0.26$) for K.

3. Ground-State PES: General Landscape and Reaction Channels along the NNO Bending Coordinate

A. Entrance and Product Channel Properties. The landscape of the ground-state PES displayed in Figure 1 is rather similar for the reactions of Li, Na, and K atoms. It comprises entrance and product valleys separated from each other by transition-state (TS) structures. Geometrical features of all relevant structures are shown in Figure 2 and listed in Table 1. Structures **I** with binding energies of 1.6, 0.1, and 1.6 kcal/mol

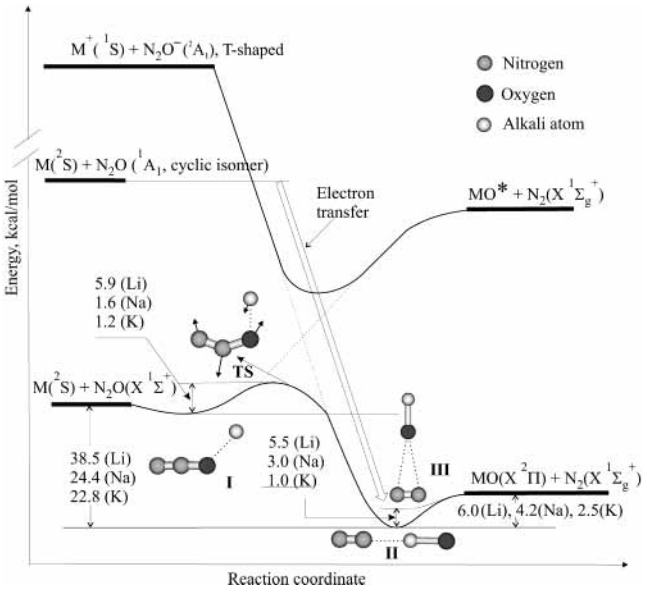

Figure 1. Potential energy profile along the lower energy channel of reaction 1.

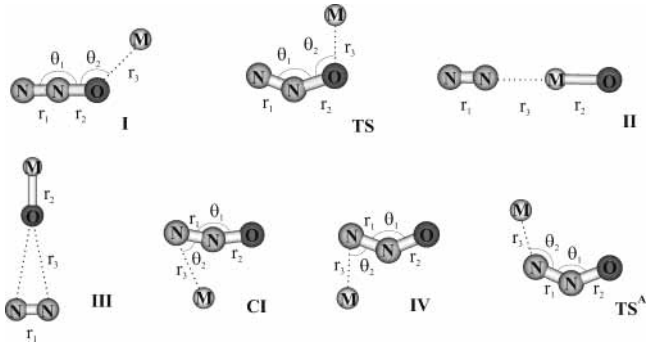

Figure 2. Key structures relevant for reaction 1. Optimized geometrical parameters are listed in Table 1.

TABLE 1: CASSCF(11/12)-Optimized Geometries for Key Structures of Reaction 1

structure[a]	r_1	r_2	r_3	θ_1	θ_2
$\mathbf{I}_{Li}$	1.115	1.210	2.154	178.6	1645
$\mathbf{I}_{Na}$	1.118	1.206	5.976	180.0	138.0
$\mathbf{I}_{K}$	1.115	1.210	3.160	179.8	151.8
TS_{Li}	1.132	1.280	1.948	147.8	104.8
TS_{Na}	1.142	1.281	2.339	146.5	98.1
TS_{K}	1.143	1.274	2.763	149.3	109.2.4
$\mathbf{II}_{Li}$	1.106	1.733	2.199		
$\mathbf{II}_{Na}$	1.107	2.110	2.631		
$\mathbf{II}_{K}$	1.107	1.246	3.279		
$\mathbf{III}_{Li}$	1.107	1.725	3.543		
$\mathbf{III}_{Na}$	1.107	2.104	3.540		
$\mathbf{III}_{K}$	1.107	2.452	3.494		
CI_{Li}	1.156	1.227	2.203	162.7	56.9
CI_{Na}	1.228	1.296	2.364	171.2	60.9
CI_{K}	1.208	1.278	2.795	168.0	57.6
$\mathbf{IV}_{Li}$	1.230	1.273	1.917	136.2	72.3
$\mathbf{IV}_{Na}$	1.228	1.290	2.312	133.9	73.8
$\mathbf{IV}_{K}$	1.221	1.303	2.719	133.5	74.2
$TS_{Li}{}^{A}$	1.207	1.284	1.821	134.2	129.4
$TS_{Na}{}^{A}$	1.206	1.288	2.147	133.7	153.5
$TS_{K}{}^{A}$	1.209	1.295	2.510	132.7	166.5

[a] See Figure 2 for the definition of the parameters. Bond lengths are given in angstroms and bond angles in degrees.

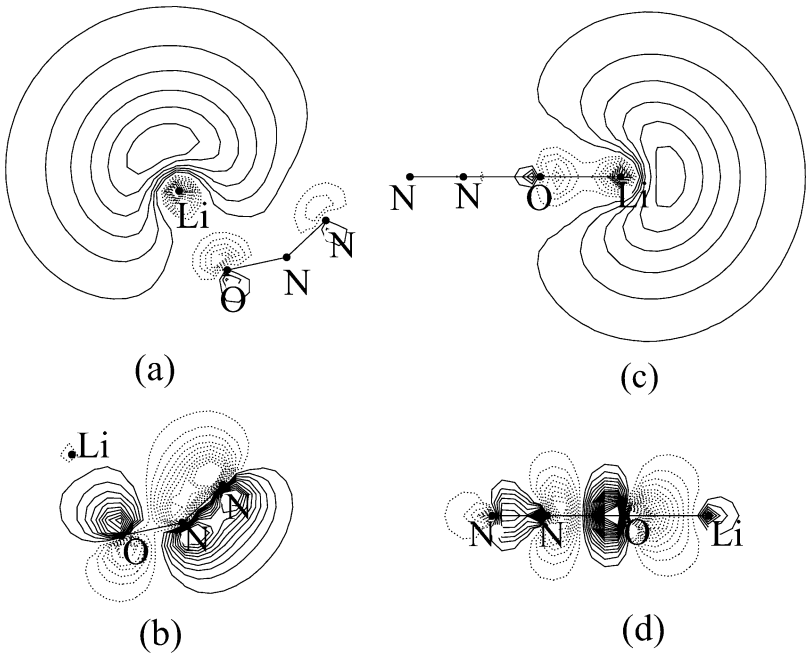

Figure 3. A representation of two different singly occupied orbitals (SOMOs) of the N_2O + Li reaction system in the two lowest electronic states that result in avoided crossing and barrier formation in "bending" and "stretching" reaction channels. The corresponding MO patterns of reaction 1 with M = Na and K are similar and not shown for compactness.

for M = Li, Na, and K, respectively, occupy a shallow minimum in the entrance channel and are only marginally stable with respect to the M + N_2O ground-state asymptote. Therein, the geometry and vibrational frequencies of the NNO moiety resemble those of the neutral nitrous oxide rather than anionic species, implying that no charge transfer occurs in the entrance channel. By way of contrast, deeper energy wells embody ionic-type complexes with linear (**II**) and T-shaped (**III**) geometries, characterized in each case by substantial charge flow from an alkali metal to oxygen. Structure **II** lies in the bottom of the product valley, representing thus the most stable arrangement of four atoms. It is slightly more stable for M = Li lying in this case 6.0 kcal/mol below the product asymptote (cf. 4.2 kcal/mol for M = Na, and 2.5 kcal/mol for M = K). The T-shaped structure **III** asymptotically correlates with a cyclic $^1A_1$ isomer of nitrous oxide that is placed ca. 63 kcal/mol[22] above the ground-state linear N_2O and does not lie on the minimum-energy reaction path.

B. Transition-State Structures. $1^2A'/2^2A'$ Avoided and Conical Intersections. Ascension from the reactant valley parallel to the doubly degenerate bending mode of N_2O, ν_2, leads to TSs that result from a lifting of the degeneracy of ν_2 due to an interaction of N_2O with M. Therefore, the lower energy reaction channel of reaction 1 is mainly determined by the normal mode ν_2. This is in accord with the earlier study on analogous Mg + N_2O,[13a] where the reaction coordinate in the transition region was also found to approximately correspond to the NNO angle, being dominated by metal−oxygen and nitrogen−oxygen distances in the entrance and product channels, respectively. Single imaginary frequencies of 1575i (TS_{Li}), 1234i (TS_{Na}), and 1920i (TS_K) characterize these transition structures describing the normal mode of predominant NNO bending character. To gain further insight into the nature and origin of the reaction barriers, we have analyzed the behavior of the two lowest electronic states, namely, $1^2A'$ and $2^2A'$, as functions of the NNO angle using a state-averaged CASSCF procedure in which equal weights were assigned to each of these states. In the reactant region, where NNO is not essentially bent, the ground $1^2A'$ state corresponds to a covalent situation of the reactants with the unpaired electron residing on the *n*s MO of a given metal, whose shape for M = Li is shown in Figure 3a, whereas the lowest lying excited state can be regarded as the charge-transfer ionic one with the unpaired electron placed on the nitrous oxide's LUMO (see Figure 3b). This picture is actually inversed for essentially bent NNO geometry ($\theta_1 < 155°$), where the ionic state becomes lower in energy than the neutral. The origin of a transition state is thus the change of predominant configuration of the electronic ground state in going from the covalent to ionic one as the NNO moiety bends. Such a change should result in an either avoided or genuine crossing between these $^2A'$ PESs. Since there is no symmetry reason for surfaces to cross at bent geometries and the states strongly mix in the transition region, the surfaces strongly "avoid" each other, giving rise to a large energy gap of ca. 25 kcal/mol in a region of closest approach for all considered M atoms. This implies that the reaction pathways along this channel are likely confined to the lowest adiabatic PES and, as a consequence, makes a "harpooning" reaction mechanism[23] extremely unlikely. The latter mechanism, involving a long-range electron transfer from a metal atom as the first step, which is, of course, an intrinsically nonadiabatic process, followed by a recombination of ions, appears to describe well the reactions of the alkaline-earth-metal atoms Ca and Sr with NO_2,[23d,24] which, in contrast to N_2O, possess sufficiently large electron affinity (3.15 eV).[25] The reaction along this channel can also be viewed as a "single-event electron transfer with atom transfer".[26]

The computed CASSCF/MR-MP2 reaction barrier heights are in line with experimental activation energies: 5.9 (3.4 ± 0.1 kcal/mol)[6a] for M = Li, 1.6 (2.8,[27a] 3.3 ± 0.4,[5c] 3.2 ± 0.1,[27b] 3.2 ± 0.8,[27c] and 3.0 ± 0.1[27d] kcal/mol) for M = Na, and 1.2 (1.2 kcal/mol)[6b] for M = K with the experimental counterparts given parenthetically. In cases of M = Li and K, where the global rate constant of reaction 1 is highly non-Arrhenius, the values shown above are derived by fitting the kinetic data with a two-channel model rate equation, where the total rate is set as the sum of two exponential functions and refers to a lower energy channel. The barriers decrease in a series from Li to its

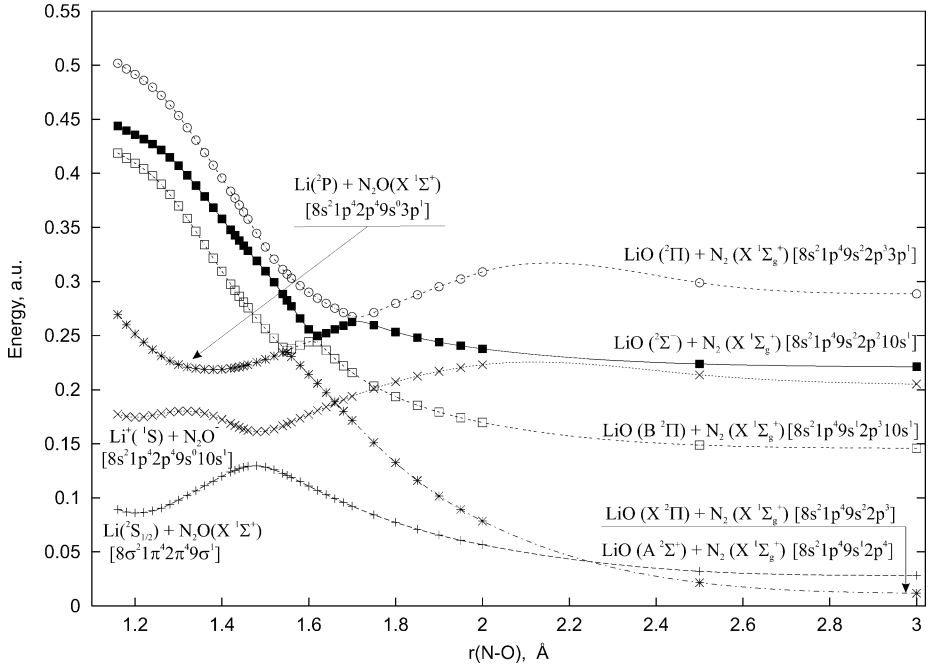

Figure 4. CASSCF(11/12) partial cross-sections of six lowest doublet electronic states for the collinear (two-dimensional) N_2O + Li reaction system as a function of the r(N−O) distance at r(Li−O) = 1.8 Å. The r(N−N) bond length is kept fixed at its experimental value in NNO of 1.1284 Å, which is justified by its small (ca. 3%) contraction going to diatomic nitrogen. Primary electron configurations of 11 active electrons are shown in brackets. The zero energy is set to the ground-state product asymptote $E_{X2\Pi} = -191.438275$ au. Analogous cross-sections for heavier congeners in a lower energy region look qualitatively similar and are not shown. They are available as Supporting Information (Figures 6S and 7S).

heavier congeners in parallel with a decrease of their ionization energies (IEs): $IE_{Li} = 5.39$, $IE_{Na} = 5.14$, $IE_K = 4.34$ eV. The Mulliken charges on metal atoms in TS structures naturally follow an opposite trend: Li (+0.1), Na (+0.28), K (+0.41). A nice empirical correlation between the sums of IEs and $s-p$ promotion energies of metals, on one hand, and the activation barriers, on the other hand, as proposed by Fontijn and co-workers[28] to rationalize the nature of the barriers in the reaction of type 1 can thus be readily understood by taking into account the fact that the metal's IEs mainly determine the reactant energy gap and hence the reaction barriers themselves in a curve-crossing model if the barriers are controlled by the interaction of neutral and ionic PESs, which, as we have shown above, is the case for reaction 1 and most likely for any radical−molecule combination.[29] As a consequence of the fact that reaction 1 involves an interaction of an open-shell with a closed-shell species, the barriers along the lowest energy channel are small, which is not, generally speaking, expected for the reaction of other kinds of metals with N_2O.

It is worth noting that the mechanism of the lower barrier formation and the energy profiles displayed in Figure 1 show a certain similarity for all the metals considered. Furthermore, regardless of the nature of M, which actually affects the barriers only quantitatively, the structural features of the NNO moiety within TS_{Li}, TS_{Na}, and TS_K are also nearly the same, displaying the θ_1 bond angle of 146.5−147.8° and an approximate 0.1 Å elongation of the N−O bond distance compared to its value in free nitrous oxide. This implies that this reaction channel is mainly determined by the nature of the NNO molecule itself and is thus reminiscent of the prototype process of dissociative electron attachment to nitrous oxide which takes place solely on the NNO PES(s).[30] This reaction channel might also be qualified as a "bending" one, due to a Renner−Teller interaction that unfolds the degeneracy of the linear $^2\Pi$ anionic state, and is likely to represent a common way for dissociation of asymmetric triatomic molecules with 16 valence electrons.[31]

The presence of same-symmetry conical intersections between the covalent and ionic PESs linking the entrance and product channels of reaction 1 is expected to be particularly interesting. Geometrical parameters of energy-minimized $1^2A'/2^2A'$ CI structures are collected in Table 1. These structures are placed 43 (CI_{Li}), 65 (CI_{Na}), and 53 (CI_K) kcal/mol above the corresponding ground-state reactant asymptotes at the CASSCF(5/6) computational level, and are characterized by a less pronounced bend ($\theta_1 \approx 163-171°$) in the NNO moiety compared to TS structures. In each of the CI structures, the alkali-metal atom is placed closer to both nitrogen atoms of NNO, as opposed to the situation in the TS, where it is linked to the NNO moiety mainly via an incipient M−O bond. Geometrically, CI structures are rather similar to the minimum-energy structures **IV** occupying shallow minima on the ionic portion of PESs, with the metal cation being nearly equally distant from both nitrogens of NNO^- and whose ionic nature could clearly be demonstrated by inspecting Mulliken charges, +0.53 ($\mathbf{IV}_{Li}$), +0.77 ($\mathbf{IV}_{Na}$), and +0.96 ($\mathbf{IV}_K$), along with molecular geometries of the *in situ* NNO (see Table 1) resembling that of the bent local minimim structure of an isolated anion. The latter structures **IV** are placed 10.9 kcal/mol below ($\mathbf{IV}_{Li}$), 4.9 kcal/mol above ($\mathbf{IV}_{Na}$), and nearly at ($\mathbf{IV}_K$) the corresponding ground-state reactant asymptotes and connected to the reaction products via TS^A structures with rather low barriers of 2.4 (TS_{Li}), 1.2 (TS_{Na}), and 0.7 (TS_K) kcal/mol on the ionic portion of the total PES.

Further examination of the energies of the $1,2^2A'$ states at a number of molecular geometries in the vicinity of CASSCF-optimized CI structures using the MCQDPT2 calculations reveals that the states remain nearly degenerate to within 1 kcal/mol; a small energy difference between the $1,2^2A'$ states arises due to the fact that only single-point calculations at this level of treatment have been performed. These calculations also suggest substantial lowering of relative energies of the CI structures with respect to the corresponding reactant asymptotes when dynamic electron correlation is taken into account. We

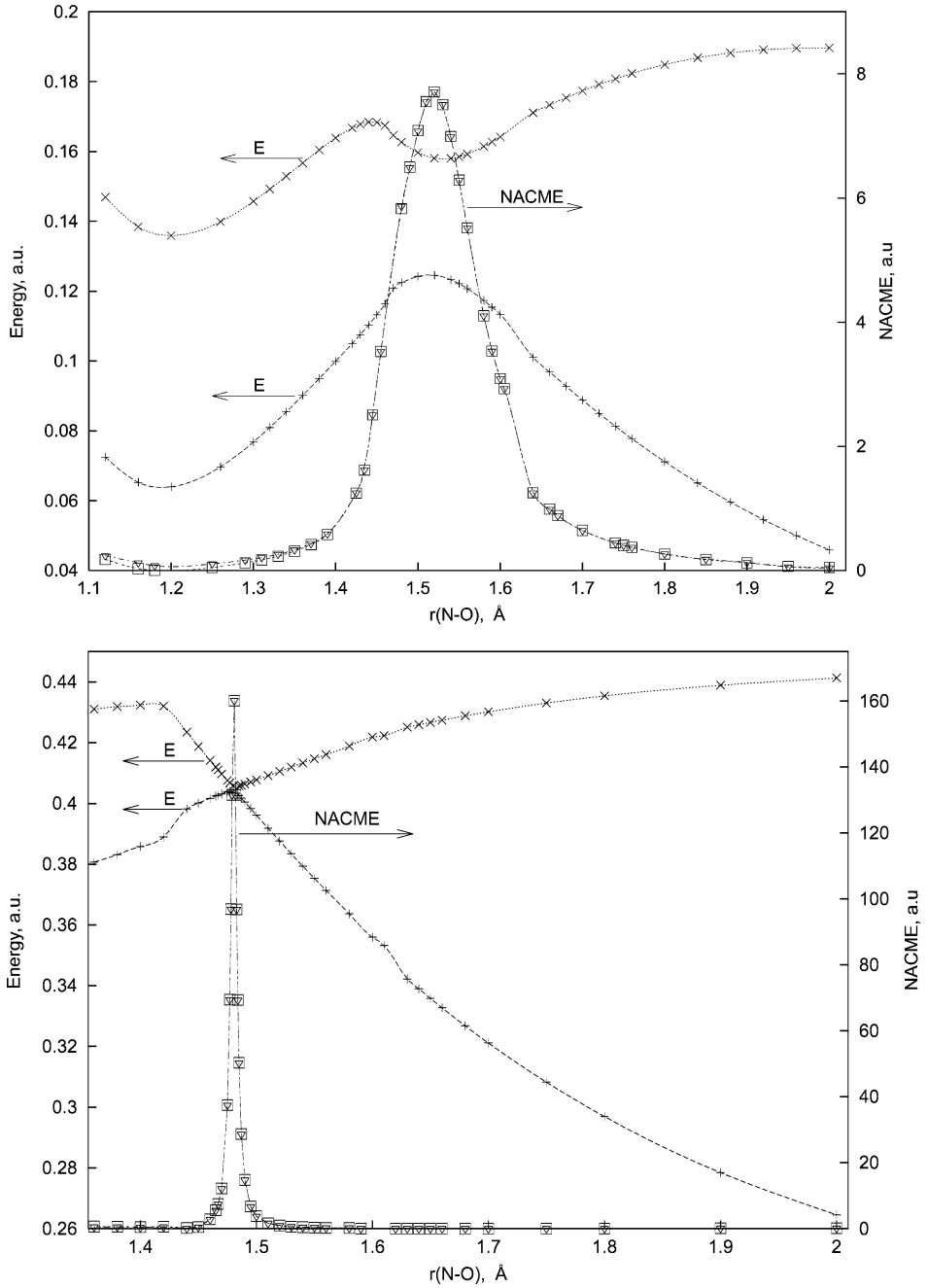

Figure 5. Nonadiabatic coupling matrix elements calculated using two-point (open triangles) and three-point (open squares) finite difference methods for the collinear NNOLi system as a function of the N−O stretching coordinate at r(Li−O) = 1.8 Å (a, top) and r(Li−O) = 1.05 Å (b, bottom). Energies of the two lower $^2A'$ states using CASSCF(11/10) are shown. The zero energy is set to the ground-state product asymptote.

therefore suggest that each reaction 1 in its non-Arrhenius regime occurs via nonadiabatic charge transfer from M to NNO along the neutral−ionic crossing in the region of the CI structures. The rest of the nonadiabatic pathway pertains to the ionic portion of PES and leads from the local minimum **IV** via TS^A to the reaction products. Speaking of the differences in observed kinetic behavior of Li, Na, and K reactions, it should be pointed out that the absence of curvature on the 1/T plot in the Na reaction does not necessarily indicate the absence of a higher energy channel in this case,[6a] but according to the present results, it could be due to the fact that CI_{Na} is located energetically higher compared to analogous structures in reaction 1 with Li and K atoms, and the contribution of a higher energy channel, even at higher temperatures, does not dominate the observed reaction rate.

4. Collinear Reaction Cross-Sections

As well-known, the reaction channels that connect reactant and product valleys always emanate from stationary points along vibrational normal modes. What we have seen so far are the reaction channels directed by the bending mode of N_2O ν_2. Apparently, there is another possibility for oxygen atom abstraction via the N_2O symmetric stretch mode ν_1, largely corresponding to the N−O stretch, which may exhibit a higher energy channel. To visualize this channel, Figure 4 displays partial cross-sections of six lowest doublet states for collinear approach of M to the oxygen side of NNO as functions of the N−O distance.

Within this channel, the electronic ground state in the reactant region has $^2A_1$ symmetry in C_{2v} (which corresponds to a $^2\Sigma$ state in $C_{\infty v}$), whereas in the product region, it possesses $^2B_1$

(or $^2\Pi$) symmetry for M = Li and Na and $^2A_1$ symmetry for M = K. Hence, the reaction in the former cases is symmetry forbidden for a collinear approach, and the ground state of the reactants asymptotically correlates with the first lower lying excited $^2\Sigma$ state of the products. The charge transfer now takes place from the metal *n*s to the antibonding σ^* orbital of the N−O bond whose shapes are shown in parts c and d, respectively, of Figure 3, and the resulting reaction barrier originates by an avoided crossing of the two lowest $^2\Sigma$ states characterized by these SOMOs. As in the case of a bending dissociation channel, there is no symmetry reason for the two surfaces to cross; however, such a crossing might occur via an accidental degeneration of these PESs. Examination of the energies of the two lower states as a function of N−O and M−O distance reveals that, as this distance decreases, these two collinear $^2\Sigma$ PESs approach each other to a distance of less than 1 kcal/mol at r(M−O) = 1.05 Å for M = Li, which is not the case for other M atoms. Taken together with a strong nonadiabatic coupling in the transition-state region which increases sharply when the r(Li−O) separation is decreased (see Figure 5), this finding indicates the possibility of a non-symmetry-related conical intersection in this region of coordinate space. The CASSCF(11/12) energy minimum structure of this CI has further been located at r(N−N) = 1.093 Å, r(N−O) = 1.479 Å, and r(Li−O) = 1.027 Å. This CI, however, is placed energetically too high, ca. 188 kcal/mol above the reactant ground-state asymptote due to a substantial amount of repulsion between O and Li atoms at such compressed geometries, and could not likely be a part of the reaction mechanism under experimental conditions described in refs 6 and 7. On the other hand, derivative coupling in the avoided crossing regions is found to be large over a wide range of r(M−O) distances, implying that the charge transfer along a higher energy nearly collinear reaction channel directed by the N−O stretching vibration occurs nonadiabatically. When looking at higher energy excited-state surfaces that are of $^2\Pi$ symmetry, a series of adjacent (narrowly avoided) crossings between them could clearly be seen, implying that the excited-state alkali-metal atom reactions M(^{2}P) + N_2O along this channel also occur on coupled PESs.

Finally, we mention that the ν_2 mode of NNO may be in Fermi resonance with the ν_1 mode,[32] implying that, at increased temperatures, their superposition may strongly affect the rate of reaction 1, giving rise to a rather unusual kinetic behavior.

5. Summarizing Remarks

The reactions of nitrous oxide with three alkali-metal atoms are investigated using ab initio electronic structure methods. In all cases considered, the lower energy portions of the ground-state PESs exibit a similar topography. The calculated energy barriers, 5.9 kcal/mol for Li, 1.6 kcal/mol for Na, and 1.2 kcal/mol for K, compare fairly well with the available experimental values determined for lower temperature ranges. These barriers are governed by strong avoided crossings between the two lower $^2A'$ PESs that change the character of the electronic ground-state wave function from a covalent dominant configuration with the unpaired electron residing on the metal's *n*s orbital to an ionic one with the latter being placed on the oxygen atom. This electron reorganization takes place at the bent geometry of the NNO moiety at an NNO bend angle of about 150°, which facilitates charge transfer. The resulting adiabatic PESs are well separated from each other, implying that the reaction apparently takes place solely on the lowest adiabatic surface. By way of contrast, the reaction along a higher energy channel takes place via nonadiabatic electron transfer from the metal atom to N_2O along the crossing of neutral and ionic PESs. This channel becomes operative at increased temperatures and likely determines the observed non-Arrhenius regime of reaction 1. Formation of the MO* luminescent products along higher energy reaction channels is also conceivable due to a close approach and strong nonadiabatic couplings between the PESs.

Acknowledgment. This work was carried out within the framework of a research project financed by the Fund for Scientific Research (FWO-Vlaanderen). The continuing support of the KU Leuven Research Council (GOA program and doctoral fellowship) is gratefully acknowledged. We also thank the reviewers for valuable suggestions.

Supporting Information Available: CASSCF(11/12) partial cross-sections of six lowest doublet electronic states for collinear N_2O + M (M = Na, K) reaction systems as functions of the r(N−O) distance (Figures 6S and 7S). This material is available free of charge via the Internet at http://pubs.acs.org.

References and Notes

(1) For a recent review see: Leont'ev, A. V.; Fomicheva, O. A.; Proskurnina, M. V.; Zefirov, N. S. *Russ. Chem. Rev.* **2001**, *70*, 91 and references therein.

(2) Prather, M.; Ehhalt, D. H. In *Climate change 2001: the Scientific Basis*; Houghton J. T., et al., Eds., Cambridge University Press: New York, 2001.

(3) Perry, R. A.; Miller, J. A. *Int. J. Chem. Kinet.* **1996**, *28*, 217.

(4) Brüning, F.; Matejcik, S.; Illenberger, E.; Chu, Y.; Senn, G.; Muigg, D.; Denifl, G.; Märk, T. D. *Chem. Phys. Lett.* **1998**, *292*, 177.

(5) (a) Wright, T. G.; Ellis, A. M.; Dyke, J. M. *J. Chem. Phys.* **1993**, *98*, 2891. (b) Plane, J. M. C.; Husain, D. *J. Chem. Soc., Faraday Trans. 2* **1986**, *82*, 2047. (c) Ager, J. W., III; Talcott, C. L.; Howard, C. J. *J. Chem. Phys.* **1986**, *85*, 5584.

(6) (a) Plane, J. M. C. *J. Phys. Chem.* **1987**, *91*, 6552, (b) Plane, J. M. C. In *Gas Phase Metal Reactions*; Fontijn, A., Ed.; Elsevier: Amsterdam, 1992; p 39.

(7) (a) Plane, J. M. C.; Rajasekhar, B. *J. Phys. Chem.* **1989**, *93*, 3135. (b) Husain, D.; Marshall, P. *Combust. Flame* **1985**, *60*, 81.

(8) Plane, J. M. C. *Int. Rev. Phys. Chem.* **1991**, *10*, 55.

(9) (a) Pfeifer, J.; Gole, J. L. *J. Chem. Phys.* **1984**, *80*, 565. (b) Woodward, J. R.; Hayden, J. S.; Gole, J. L. *Chem. Phys.* **1989**, *134*, 395.

(10) (a) Langhoff, S. R.; Partridge H.; Bauschlicher, C. W., Jr. *Chem. Phys.* **1991**, *153*, 1. (b) Serrano-Andrés, L.; de Merás, A. S.; Pou-Amérigo, R.; Nebot-Gil, I. *Chem. Phys.* **1992**, *162*, 321.

(11) Brekenridge, W. H.; Fournier, P.-R.; Gaveau, M.-A.; Mestagh, J.-M.; Visticot, J.-P. *Chem. Phys. Lett.* **2002**, *364*, 225.

(12) (a) Stirling, A. *J. Phys. Chem. A* **1998**, *102*, 6566. (b) Delabie, A.; Vinckier, C.; Flock. M.; Pierloot, K. *J. Phys. Chem. A* **2001**, *105*, 5479. (c) Stirling, A. *J. Am. Chem. Soc.* **2001**, *124*, 4058. (d) Kryachko, E. S.; Tishchenko, O.; Nguyen, M. T. *Int. J. Quantum Chem.* **2002**, *89*, 329.

(13) (a) Yarkony, D. R. *J. Chem. Phys.* **1983**, *78*, 6763. (b) Kiran, B.; Vinckier, C.; Nguyen, M. T. *Chem. Phys. Lett.* **2001**, *344*, 213.

(14) Tishchenko, O.; Kryachko, E. S.; Vinckier C.; Nguyen, M. T. *Chem. Phys. Lett.* **2002**, *363*, 550.

(15) (a) Ruedenberg, K.; Schmidt, M. W.; Gilbert, M. M.; Elbert, S. T. *Chem. Phys.* **1982**, *71*, 41. (b) Roos, B. O.; Taylor, P.; Siegbahn, P. A. E. *Chem. Phys.* **1980**, *48*, 157. (c) Werner, H.-J.; Knowles, P. J. *J. Chem. Phys.* **1985**, *82*, 5053. (d) Knowles, P. J.; Werner, H.-J. *Chem. Phys. Lett.* **1985**, *115*, 259.

(16) (a) Hirao, K. *Chem. Phys. Lett.* **1992**, *190*, 374. (b) Hirao, K. *Chem. Phys. Lett.* **1992**, *196*, 397. (c) Hirao, K., *Ibid.* **1993**, *201*, 59. (d) Hirao, K. *Int. J. Quantum Chem.* **1992**, *S26*, 517. (e) Nakano, H., *J. Chem. Phys.* **1993**, *99*, 7983.

(17) Schmidt, M. W.; Gordon, M. S. *Annu. Rev. Phys. Chem.* **1998**, *49*, 233.

(18) Werner, H.-J.; Follmeg, B.; Alexander, M. H. *J. Chem. Phys.* **1988**, *89*, 3139.

(19) MOLPRO is a package of ab initio programs designed by H.-J. Werner and P. J. Knowles, version 2002.1: Amos, R. D.; Bernhardsson, A.; Berning, A.; Celani, A.; Cooper, D. L.; Deegan, M. J. O.; Dobbyn, A. J.; Eckert, F.; Hampel, C.; Knowles, P. J.; Korona, T.; Lindh, R.; Lloyd, A. W.; McNicholas, S. J.; Mandy, F. R.; Meyer, W.; Mura, M. E.; Nicklass, A.; Palmieri, P.; Pitzer, R.; Rauhut, G.; Schütz, M.; Schumann, U.; Stoll, H.; Stone, A. J.; Tarroni, R.; Thorsteinsson, T.; Werner, H.-J.20. Schmidt,

M. W.; Baldridge, K. K.; Boatz, J. A.; Elbert, S. T.; Gordon, M. S.; Jensen, J. H.; Koseki, S.; Matsunaga, N.; Nguyen, K. A.; Su, S. J.; Windus, T. L.; Dupuis, M.; Montgomery, J. A. *J. Comput. Chem.* **1993**, *14*, 1347.

(20) Schmidt, M. W.; Baldridge, K. K.; Boatz, J. A.; Elbert, S. T.; Gordon, M. S.; Jensen, J. H.; Koseki, S.; Matsunaga, N.; Nguyen, K. A.; Su, S. J.; Windus, T. L.; Dupuis, M.; Montgomery, J. A. *J. Comput. Chem.* **1993**, *14*, 1347.

(21) Wachters, A. J. H. *J. Chem. Phys.* **1970**, *52*, 1033.

(22) Hopper, D. G. *J. Chem. Phys.* **1984**, *80*, 4290.

(23) (a) Polanyi, M. *Atomic reactions*; Williams and Norgate, Ltd.: London, 1932. (b) Evans M. G.; Polanyi, M. *Trans. Faraday Soc.* **1939**, *35*, 1753. (c) Polanyi, M. *Endeavor* **1949**, *8*, 3. (d) Herschbach, D. R. *Adv. Chem. Phys.* **1966**, *10*, 319.

(24) (a) Vinckier, C.; Helaers, J.; Christiaens, P.; Remeysen, J. *J. Phys. Chem. A* **1999**, *103*, 11321. (b) Jonah, C. D.; Zare, R. N.; Ottinger, C. *J. Chem. Phys.* **1972**, *56*, 263.

(25) (a) Warneck, P. *Chem. Phys. Lett.* **1969**, *3*, 532. (b) Wagner, O. E. *Bull. Am. Phys. Soc.* **1968**, *13*, 1395.

(26) Cannon, R. D. *Electron Transfer Reactions*; Butterworth: London, 1980; p 29.

(27) (a) Worsnop, D. R.; Zahniser, M. S.; Kolb, C. E. *J. Phys. Chem.* **1991**, *95*, 3960. (b) Demore, W. B.; Sander, S. P.; Golden, D. M.; Hampson, R. F.; Kurylo, M. J.; Howard, C. J.; Ravishankara, A. R.; Kolb, C. E. JPL-Publication 97-4; 1997. (c) Husain, D.; Marshall, P. *Combust. Flame* **1985**, *60*, 81.

(28) Fontijn, A.; Futerko, P. M. In *Gas Phase Metal Reactions*; Fontijn, A., Ed.; Elsevier: Amsterdam, 1992; p 93 and references therein.

(29) Donahue, N. M.; Clarke, J. S.; Anderson, J. G. *J. Phys. Chem. A* **1998**, *102*, 3923.

(30) Kryachko, E. S.; Vinckier, C.; Nguyen, M. T. *J. Chem. Phys.* **2001**, *114*, 7911.

(31) Suzuki, T.; Katayanagi, H.; Nanbu, S.; Aoyagi, M. *J. Chem. Phys.* **1998**, *109*, 5778.

(32) Herzberg, G. *Molecular Spectra and Molecular Structure, Vol II, Infrared and Raman Spectra of Polyatomic Molecules*; Krieger Publishing Co.: Malabar, FL, 1991; p 277.